Journal of Power Sources 186 (2009) 194–200

Contents lists available at ScienceDirect

Journal of Power Sources

journal homepage: www.elsevier.com/locate/jpowsour

Preparation and electrochemical performance of ultra-short carbon nanotubes

Xiao X. Wang[a,b], Jian N. Wang[a,b,*], Lian F. Su[a,b]

[a] School of Materials Science and Engineering, Tongji University, 1239 Siping Road, Shanghai 200092, PR China
[b] School of Materials Science and Engineering, Shanghai Jiao Tong University, 800 Dong Chuan Road, Shanghai 200240, PR China

ARTICLE INFO

Article history:
Received 10 June 2008
Received in revised form
15 September 2008
Accepted 19 September 2008
Available online 30 September 2008

Keywords:
Short carbon nanotubes
Preparation
Li-ion battery
Fuel cell

ABSTRACT

Current carbon nanotubes (CNTs) are typically synthesized with micrometer lengths, low dispersion and low purity and thus oppose their applications in many fields. In this study, we make the first report on using a Fe compound (FeS) as a catalyst for controlling the length of CNTs to be less than 300 nm. This is achieved by dissolution of a proper proportion of ferrocene and thiophene in alcohol and pyrolysis of this solution at high temperature. Sulfur, resulting from the decomposition of thiophene, is shown to play key roles in promoting the growth of CNTs and limiting their length. The reason is suggested to be that FeS retards the dissociation of carbon source and diffusion of carbon in it as compared with pure Fe. Short CNTs from the present direct synthesis and from our previous solid-state cutting are used as an electrode material in Li-ion batteries and catalyst supports in fuel cells. Compared with conventional long CNTs, short CNTs show much better electrochemical performance. Due to the simplicity of the present synthetic technique, it may be used for mass production of short CNTs. Furthermore, the application of such a new material may be investigated in wide areas such as information technology, biomedicine, environmental and energy industries.

1. Introduction

Since the landmark paper on carbon nanotubes (CNTs) [1], they have attracted much attention on many applications because of their unique mechanical, physical and chemical properties [2,3]. However, before these properties can be fully used, several technical hurdles must be overcome. One of such hurdles concerns the length control. Current CNTs are typically synthesized with micrometer lengths where they are bound into macroscopically entangled ropes or masses. This contradicts with the requirements of many projected applications for short and highly dispersed CNTs with lengths of a few hundred nanometers or less. For example, CNT agglomerates do not provide the three-dimensional networks needed to efficiently carry mechanical loads or provide useful transport properties for a composite. Highly entangled CNTs that are difficult to disperse uniformly in fluids and melts would give fluid suspensions and composites that have only slight improvements in their mechanical or transport properties. In meantime, highly entangled CNTs cannot show their advantage of high surface area and hollow inner space. Thus, exploration of CNTs with a short length and high dispersion is of paramount scientific and technological importance and would fill the large gap between small spheroidal fullerenes and long CNTs.

In order to prepare short CNTs, a number of cutting methods have been practiced to shorten long ones either mechanically, chemically, or as a combination of these. Mechanical cutting is induced by ball-milling [4,5] or sonication with an abrasive [6]. Chemical cutting is achieved by partially functionalizing the tubes with fluorine and then pyrolysis at high temperature [7]. A combination of mechanical and chemical cutting is ultrasonically induced cutting in an oxidizing acid [8,9]. But these cutting processes often involve destruction of the graphitic structure, inhomogeneous cutting with remaining long CNTs, difficulty in elimination of the impurities such as amorphous carbon produced, and a significant loss of raw material (50 wt.% or even higher). Recently, a new approach was reported to cut the conventional long and entangled CNTs by depositing NiO [10] or Fe_2O_3 [11] particles on CNTs first and then inducing a chemical reaction between them at high temperature. This cutting approach based on such a solid-state reaction has advantages of producing CNTs with a short length (<300 nm), a narrow length distribution, high dispersion, and a low material loss over previous ones based on a gaseous or liquid-state reaction.

There have been many reports about the synthesis of CNTs using Fe as catalyst and sulfur to enhance the growth. But the CNTs obtained always have long lengths of several micrometers. Direct synthesis of short CNTs has appeared difficult. This is because the

* Corresponding author at: School of Materials Science and Engineering, Tongji University, 1239 Siping Road, Shanghai 200092, PR China. Fax: +86 21 65985385.
E-mail address: jnwang@mail.sjtu.edu.cn (J.N. Wang).

0378-7753/$ – see front matter © 2008 Elsevier B.V. All rights reserved.
doi:10.1016/j.jpowsour.2008.09.074

growth rate of CNTs is very fast using the current techniques of laser ablation, arc discharge, and chemical vapor deposition (CVD) [2]. For example, using carbon isotope labeling, the growth rate in catalytic CVD was measured to be 360 nm s^{-1} at 690 °C but 820 nm s^{-1} at 710 °C [12]. For the current synthesis of CNTs, nanometer-sized metal particles are usually present. It is generally believed that such catalytic growth involves the decomposition of carbon-containing gas on one side of a catalyst particle, subsequent diffusion of carbon atoms through the volume or surface of the particle, and then precipitation of CNT on its other side [13,14]. Since the diffusivity of carbon in catalyst particles apparently affects the growth rate of CNTs, conventional fast growth may be suppressed and short CNTs may be synthesized if a new catalyst with a low diffusivity of carbon is used. An immediate consideration for such a catalyst may be a compound of the widely used transition metal of Fe, Ni or Co.

To test the above idea, we explored the feasibility of using an iron compound as the catalyst for growing CNTs and controlling the length. FeS was chosen to be used as a catalyst since they can be obtained from ferrocene and thiophene easily. We give the first report on a simple but effective technique involving FeS for direct synthesis of short and high-dispersion CNTs. This technique takes the advantages of floating catalyst and the use of alcohol as the carbon source. That is, both ferrocene and thiophene are dissolved in alcohol and the solution is sprayed into the reaction zone. Thiophene is added at such a high quantity that FeS is formed. As will be shown, it is convenient to continuously produce short and highly dispersed CNTs. When such short CNTs are used as an electrode material in Li-ion batteries and a catalyst support in fuel cells, they are found to show much better performance than conventional long CNTs.

2. Experimental

2.1. Preparation

Short CNTs were synthesized by spray pyrolysis. The experimental setup consisted of an electric furnace, a quartz tube (30 mm in inner diameter and 1.2 m in length), and a sample collector. A quartz capillary was used for solution supply and spraying. Ferrocene and thiophene were dissolved in ethanol at a concentration of 20 g L^{-1} and 50 mL L^{-1}, respectively. In a typical experiment, the quartz tube was flushed with Ar first in order to eliminate oxygen from the reaction chamber, and then heated to a temperature from 950 to 1100 °C. After 15 min holding at the temperature, Ar flow was initiated at a rate of 120 L h^{-1}. Subsequently, the ethanol solution was supplied by an electric squirming pump. The supplying rate was adjusted to be 50 mL L^{-1}. After a few hours, the supply of ethanol was terminated and the reaction chamber was cooled gradually to room temperature. Pyrolysis products were collected in a glass bottle connected to the quartz tube. The as-grown samples were purified in an acid solution at 110 °C for about 1 h to remove ferrous particles. The acid used was a concentrated HNO_3 with a concentration of 65 wt.%. But this acid was diluted by an equal volume of H_2O before use.

2.2. Characterization

X-ray diffraction (XRD) experiments were conducted on different CNT samples. The X-ray diffractometer (Bruker D8 Advance, Bruker AXS, Germany) was operated at 40 kV and 40 mA. Nickel-filtered Cu Kα radiation was used in the incident beam. Transmission electron microscopy (TEM, JEM-100CX) was used to study the microstructure and morphology of long and short CNTs. The samples were dispersed in ethanol by means of a sonicator and scooped up with an amorphous carbon film for TEM observations. High resolution TEM (HRTEM, JEM-2010F, accelerating voltage 200 kV) and energy dispersive spectrum (EDS) were used to study the structure of CNTs and the chemical compositions of particles at the tips of CNTs. Raman spectroscopy was recorded using an Ar^+ ion laser at 514.5 nm wavelength (Renishaw InVia plus, Renishaw plc, U.K.) to assess the graphitic structure of CNTs. The main features in the Raman spectrum are the disorder-induced D band at 1350 cm^{-1} and the G band corresponding to the graphitic structures at 1580 cm^{-1}. The intensity ratio of these bands was calculated giving a semi-quantitative indication of the defect concentration in nanotubes. Thermogravimetric analysis was performed using a Diamond TG/DTA 6300 instrument in an atmosphere of air.

2.3. Electrochemical test

The electrochemical properties of short and long CNTs as anodes in Li-ion cells were evaluated. The cells for charge/discharge tests consisted of Li foils as reference and counter electrodes and CNTs as working electrodes. The working electrodes were prepared by coating a slurry consisting of 90 wt.% active material, 5 wt.% Super P as conductive substance, and 5 wt.% polytetrafluoroethylene (PTFE) as binder on a foam Ni plate. Then, the foam Ni plate was hydraulically pressed into 0.3 mm thickness under a pressure of 6 MPa. All the electrodes were dried for 12 h at 120 °C in vacuum, and had a total weight of 3–5 mg. The electrolyte used was 1 M of $LiPF_6$ dissolved in a 1:1 by volume of ethylene carbonate (EC) and dimethyl carbonate (DMC) mixture. The Li/CNT cells were assembled as coin types in an argon-filled glove box (O_2 < 1 ppm, H_2O < 1 ppm). Galvanostatical charge and discharge were controlled between 0.005 and 3.0 V vs. Li/Li^+ on a cell test instrument (LAND CT2001 A, Wuhan Kingnuo Electronic Co., China) at ambient temperature.

For the application as the catalyst support in fuel cells, Pt nanoparticles were deposited on long and short CNTs. In a typical experiment, CNTs were sonicated in ethylene glycol to form slurry, which was heated up to a desired temperature around 140 °C. Then, chloroplatinic acid (H_2PtCl_6) dissolved in ethylene glycol was dropped slowly into the CNT slurry. The ethylene glycol here acts both as a reducing medium as well as a surfactant preventing the conglomeration of Pt nanoparticles. The reaction mixture was refluxed for 3 h at 140 °C. After cooling to room temperature, the Pt/CNT catalyst was filtered, washed with deionized water and dried for following tests.

The electrochemical activities of the catalysts were characterized by cyclic voltammetry (CV) technique in a conventional three-electrode cell at ambient temperature. To prepare a work electrode, the catalyst was ultrasonically mixed with ethanol and 5% Nafion isopropanol solution for 30 min first. The slurry was then coated on a glassy carbon cylinder with a diameter of 3 mm. The amount of catalyst loading on the electrode was controlled to be 0.4 mg cm^{-1}. A saturated calomel electrode (SCE) and a large-area Pt plate were used as the reference electrode and counter electrode, respectively, and 0.5 M H_2SO_4 was used as the electrolyte. The CV profiles were recorded at a scan rate of 100 mV s^{-1} from the potential of −0.24 to 1.0 V vs. SCE.

3. Results and discussion

3.1. Direct growth of short CNTs

Direct growth of short CNTs involved FeS-catalyzed pyrolysis of ethanol. Fig. 1a shows the TEM image of the sample synthesized at 1100 °C with the ferrocene and thiophene concentrations being 20 g L^{-1} and 50 mL L^{-1}, respectively. It can be seen that CNTs are

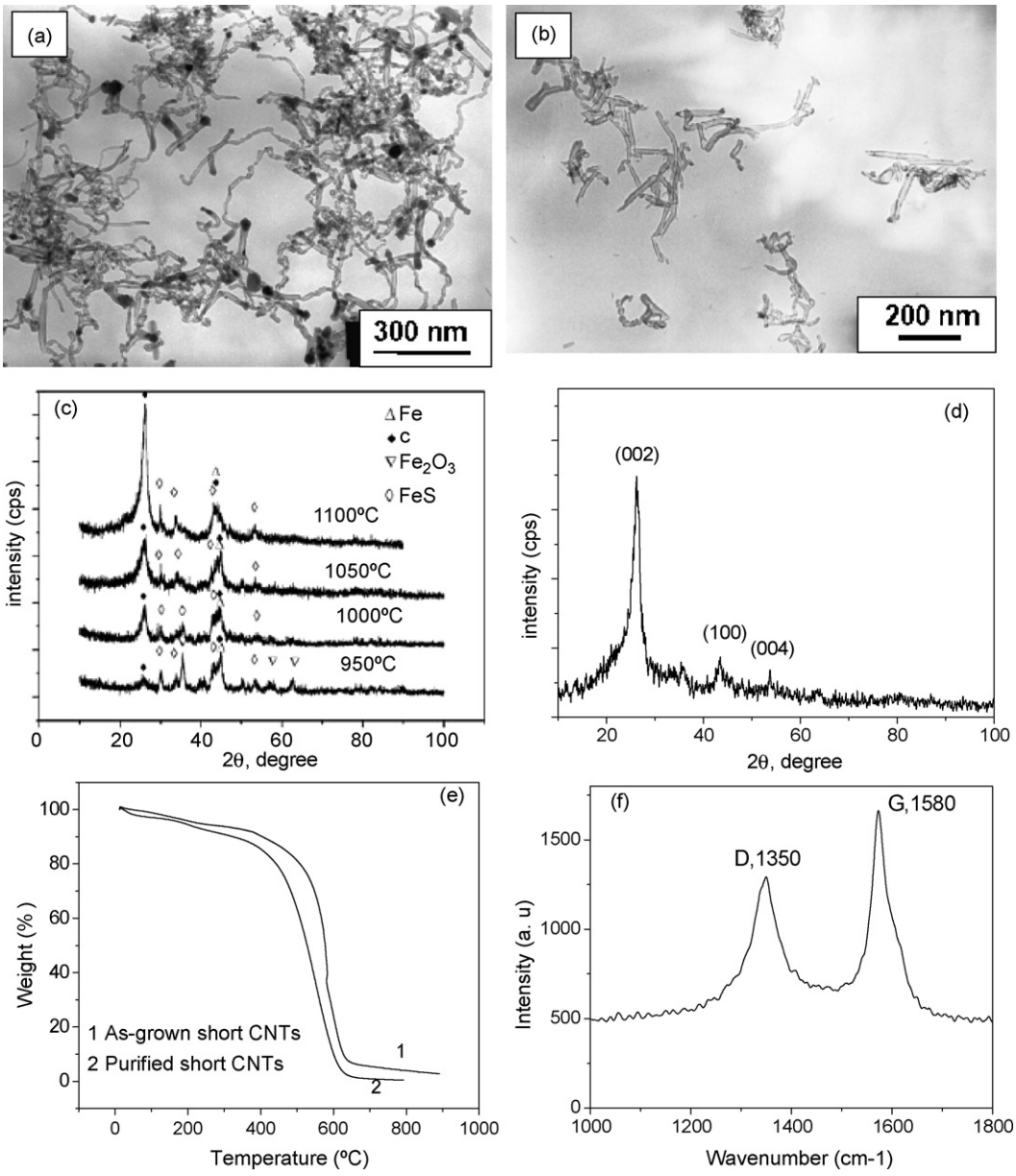

Fig. 1. TEM images and XRD patterns of the as-grown (a and c), and purified (b and d) short CNTs. *Note*: the presence of FeS in samples prepared at different temperatures. Fe_2O_3 may result from the oxidation of ferrous phases. TG curves of the as-grown and purified short CNTs (e) and Raman spectrum of purified short CNTs (f).

about 200–500 nm in length and 20–30 nm in diameter. At the tips of most CNTs, there are catalytic particles. After purification, CNTs are open at both ends and have lengths generally less than 300 nm. They are highly dispersed and do not form large agglomerates in the whole sample (Fig. 1b). XRD analyses elucidate the presence of FeS in all samples (Fig. 1c), and with increasing temperature, the peak for FeS becomes stronger. At the same time, the peak of Fe is very weak, suggesting that there are few Fe catalytic particles in the samples. After purification, only graphite peaks could be identified (Fig. 1d), indicating complete elimination of ferrous particles. This observation is supported by thermogravimetric analysis (Fig. 1e). For the as-grown sample, FeS might have reacted with oxygen and generated iron oxide. This may be responsible for the residual weight observed. But for the purified sample, no residual weight is observed after complete oxidation, suggesting that FeS had been removed completely during purification. The result from Raman spectrum shows that the ratio of the intensity of the G mode to that of the D mode (I_G/I_D) is about 1.3, and thus also suggests that the short CNTs have a good graphitic structure (Fig. 1f).

Detailed HRTEM and EDS studies of as-grown CNTs are presented in Fig. 2. As shown, the short CNTs are made up of graphitic layers, and the particle encapsulated at the tip also has a crystalline structure and contains Fe and S with an atomic ratio of 1:1. The interplanar spacing was measured to be about 0.3 nm, which is consistent with the spacing for (2 0 0) plane of FeS. The Cu peak originated from the Cu grid used for preparation of TEM sample. This observation suggests that the particle encapsulated is probably FeS.

Thiophene concentration was found to have a profound effect on the experimental result. In the case that no thiophene was added, the sample consisted of mainly long nanofibers (>1 μm) and some Fe nanoparticles embedded in the fibers with very few CNTs (Fig. 3a). With the addition of thiophene of 30 mL L^{-1}, the sample contained both long carbon fibers as in the sample without

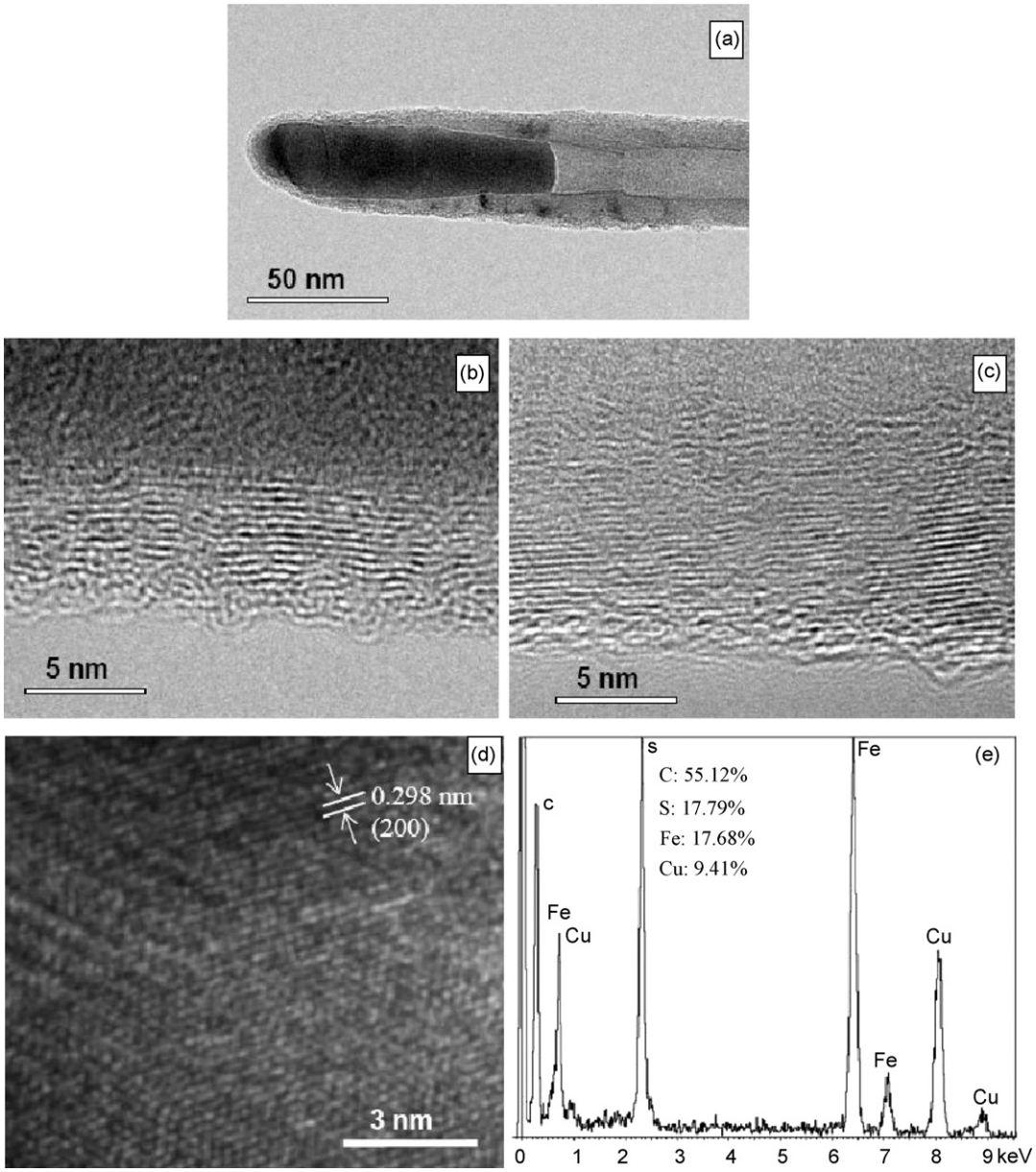

Fig. 2. TEM image of an as-grown CNT with an encapsulated particle (a), lattice fringes of the encapsulating layer (b), the tube wall (c) and the particle (d), and EDS of the particle (e).

thiophene addition and short CNTs as in the sample with the addition of thiophene of 50 mL L^{-1} (Fig. 1). In the case that a high thiophene concentration of 100 mL L^{-1} was introduced, the sample included carbon particles only (Fig. 3b).

3.2. Origin of Short CNTs

The present study provides first evidence that when a high content of thiophene was added (50 mL L^{-1} in the present system), FeS formed as shown by XRD (Fig. 1c) and EDS (Fig. 2e). The formation of FeS promoted the growth of CNTs instead of CNFs and limited their lengths to be less than 300 nm. In previous studies, however, a much lower content of thiophene was included and the formation of FeS was not identified. Although the growth of CNTs was also promoted, their lengths were in the range of micrometers [15,16].

Now the origin of the important role played by sulfur in promoting the growth of CNTs in the present experiments is considered. It is well known that Fe is a very active catalyst for the growth of carbon nanofibers at 1100 °C (Fig. 3a). Its activeness might be so high that the catalytic pyrolysis of hydrocarbon molecules could be very fast and sufficient carbon might be generated for the growth of nanofibers. When thiophene was added, however, sulfur atoms could combine with Fe atoms to form FeS at high temperature. This would decrease the catalytic activity of Fe particles and the decomposition of alcohol. Consequently, fewer carbon atoms were produced and the growth of CNTs was favored (Fig. 1).

In addition to the activity of the catalytic particle, the size of the catalytic particle should be also considered as a factor determining the growth of nanofibers or nanotubes. A previous study showed that the product consisted of nanofibers when the size of the metal particle was above 20 nm but nanotubes when the size of the metal particles was less than 20 nm [17]. The addition of sulfur could induce the fragmentation of metal particles and thus be favorable for growing CNTs (Fig. 1).

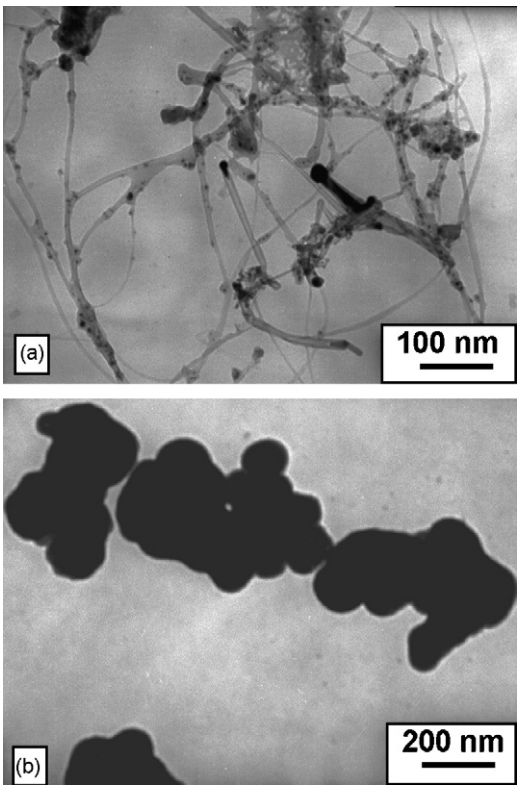

Fig. 3. TEM images of the carbon nanofibers (a) and carbon particles (b) synthesized without and with 100 mL L^{-1} thiophene additions, respectively. Compare these samples with the short CNT sample synthesized with 50 mL L^{-1} thiophene addition shown in Fig. 1.

The second important role played by sulfur is its effect on limiting the length of CNTs. Unlike the previous CNTs with lengths in the micrometer range, the present CNTs have lengths in the nanometer range (Fig. 1). A number of previous studies suggested that the growth rate of CNTs is very fast [2,11]. The growth may be considered to consist of processes of dissolution, diffusion and precipitation of carbon atoms in the catalytic particle. With the formation of FeS, all these processes would be much slower than in pure Fe. This could result in an overall growth rate much slower than that for the pure Fe case. Considering the gas flow rate of 120 L h^{-1}, heating length of ~70 cm, reactor diameter of ~3 cm, and CNT length of ~300 nm, the growth rate is estimated to be ~20 nm s^{-1} in the present experiment. This rate is more than one order of magnitude slower than previously reported values.

However, it should be noted that superfluous sulfur atoms could cover the entire surface of a catalytic particle and prevent the decomposition of alcohol and the adsorption of carbon atoms on the catalytic particle. In this case, CNTs could not grow and carbon atoms could only be adsorbed on the catalytic particle to form carbon spheres. The observed carbon particles with the addition of a high content of thiophene (100 mL L^{-1}) (Fig. 3b) might have this origin.

Except for some catalytic particles which can be easily removed with mild purification, the present CNTs were produced in high purity without H_2. The reason why the alcohol is a better carbon source for CNTs than other hydrocarbons may be related to the role of decomposed OH radicals as suggested before [18]. It is known that an OH radical efficiently eliminates the amorphous carbon in the purification process of CNTs using H_2O_2 [19]. Since an OH radical from an alcohol molecule is decomposed on the catalyst surface, it will attack nearby carbon atoms with a dangling bond to form CO. Then, seeds of amorphous carbon are efficiently removed in its very early stage. Hence, the OH radical prohibits the generation of byproducts, and only the CNTs can survive under this condition.

3.3. Applications of short CNTs

To show their potential applications, the present short CNTs from direct growth are used as an electrode material in Li-ion batteries and a catalyst support in fuel cells. For comparison, conventional long CNTs and the short ones from our solid-state cutting [11] are also included. Fig. 4a and b illustrate the TEM images of these CNTs. The long CNTs have a diameter of 20–30 nm and a length in the range of 1–5 μm. However, after cutting, CNTs with a short length of ~300 nm and good dispersion are obtained (Fig. 4b). Many analyses showed that the solid-state cutting induced little destruction of the graphitic structure and a low material loss of ~15 wt.% [11].

3.3.1. Application in Li-ion battery

The short CNTs from direct growth, the cut ones, as well as the conventional long ones were used as electrode materials in Li-ion batteries. Fig. 5a–c show the first two cycles of discharge and charge curves of these three different CNT materials at a current density of 25 mA g^{-1}. The reversible capacity (C_{rev}) is defined as the charge capacity in the first cycle, and the irreversible capacity (C_{irr}) is the difference in capacity between the first discharge and the first charge, resulting from the decomposition of electrolyte to form solid electrolyte interface (SEI). From Fig. 5, it can be seen that the C_{rev} for the long CNTs is 188 mA h g^{-1}, but those for the short CNTs and the cut ones are 502 and 577 mA h g^{-1}, respectively. Evidently, the C_{rev} increases significantly with shortening the length of CNTs. At the same time, the irreversible capacities for both short and cut CNTs increased, which may be associated with the open ends,

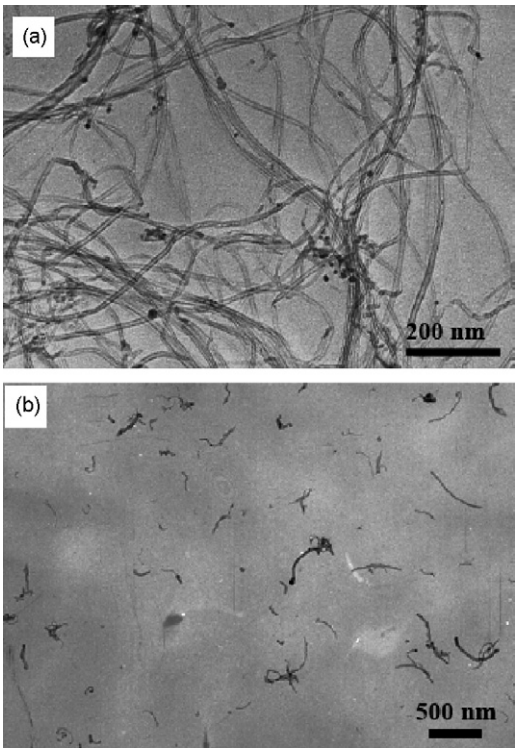

Fig. 4. TEM images of conventional long CNTs (a) and the cut CNTs from solid-state reaction (b).

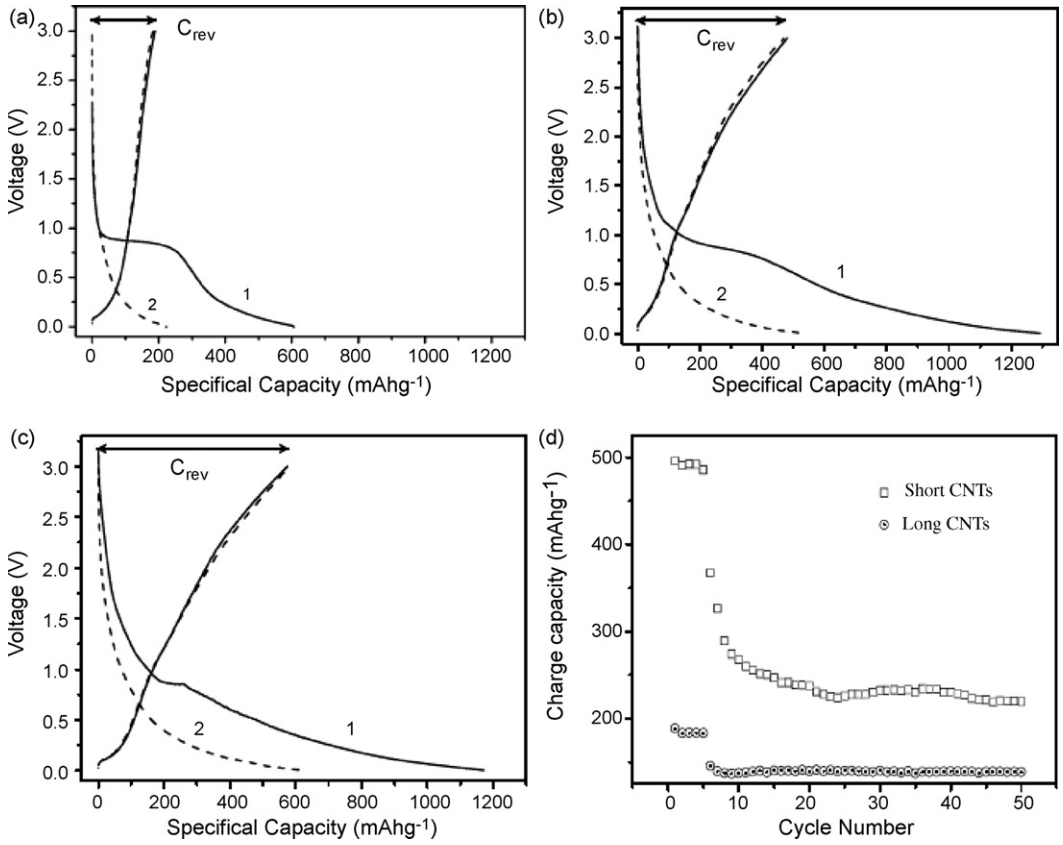

Fig. 5. Performance of different CNTs in Li-ion batteries. Discharge/charge curves of Li insertion/extraction into/from conventional long (a), short (b), and cut CNTs (c) for the first and second cycles at a current density of 25 mA g^{-1}, and charge capacities of long and short CNTs as a function of cycle number (d).

shortened length and increased surface area. The initial coulombic efficiency (CE) for the long CNTs was 31% but about 40–49% for the short CNTs. It can be seen that the CE of short CNTs increased, in spite of a higher C_{irr}.

The charge capacities of long and short CNTs as a function of cycle number are shown in Fig. 5d. It can be clearly seen that the short CNTs have a higher lithium extraction capacity than the long CNTs. After 20 cycles, the charge capacity becomes stable. This stable capacity is about 230 mAh g^{-1} for the short CNTs but 142 mAh g^{-1} for the long CNTs, suggesting a better cyclic performance for the short CNTs.

The short CNTs and the cut ones show similar electrochemical properties which are much better than those for the conventional long CNTs. The reason for this may be that the insertion/extraction of Li ions into/from short CNTs is facilitated by the shortened length of the tubes. Moreover, short CNTs have much more edges (open ends) than long CNTs per unit length. Thus, it would be much easier for Li ions to intercalate/deintercalate into/form the graphitic sheets in short CNTs than those in long CNTs, thus showing higher reversible and irreversible capacities.

3.3.2. Application in fuel cell

The present CNTs are also used as a catalyst support for proton exchange membrane fuel cells. Fine Pt particles are found to uniformly deposit on all CNT materials. A typical example is shown in Fig. 6a for the case of the short CNTs. XRD patterns show that Pt particles deposited on all CNT materials have the same exposed lattice planes (Fig. 6b). The mean size of Pt particles is estimated to be about 4 nm on all CNT materials from the Scherer's formula (Table 1).

Fig. 6c illustrates the electrochemical activities of the prepared catalysts with a Pt deposition of 45 wt.%. As can be seen, the Pt catalysts based on short and cut CNTs demonstrate much higher hydrogen desorption/adsorption peaks and thus much higher activities than the Pt catalyst based on long CNTs. Calculations based on the cyclic voltamograms (Fig. 6c) show that the electroactive

Table 1
List of the characteristics of different CNT-based catalysts.

Samples	Pt particle size (nm)[a]	Pt surface area ($m^2\ g^{-1}$)[b]	Electroactive surface area ($m^2\ g^{-1}$)[c]	Pt utilization ratio (%)[d]
Pt/long CNTs	4.14	67.7	17.3	25.5
Pt/cut CNTs	3.65	76.8	33.4	43.5
Pt/short CNTs	3.92	71.5	24.8	34.7

[a] $L_c = 0.9\lambda/(\beta\cos\theta)$, where L_c is average crystallite size, λ the X-ray wavelength, θ the (2 2 0) peak position, and β represents FWHM value.

[b] $S = 6000/\rho L_c$, where L_c is average crystallite size (nm), S the surface area ($m^2\ g^{-1}$), and ρ represents Pt density (21.4 g cm^{-3}).

[c] $\alpha = Q/(m\beta)$, where α is the electroactive surface area of Pt ($m^2\ g^{-1}$), Q the charge for hydrogen desorption without the contribution from the electric double layers marked with shadow in Fig. 4c (mC cm^{-2}), m the quantity of Pt used (=0.4×10^{-3} g cm^{-2} in the present study), and β the charge required to oxidize a monolayer of H_2 on bright Pt (=0.21 mC cm^{-2}).

[d] $u = \alpha/S$, where u is the utilization ratio of Pt, α is the electroactive surface area ($m^2\ g^{-1}$), and S the surface area of Pt ($m^2\ g^{-1}$).

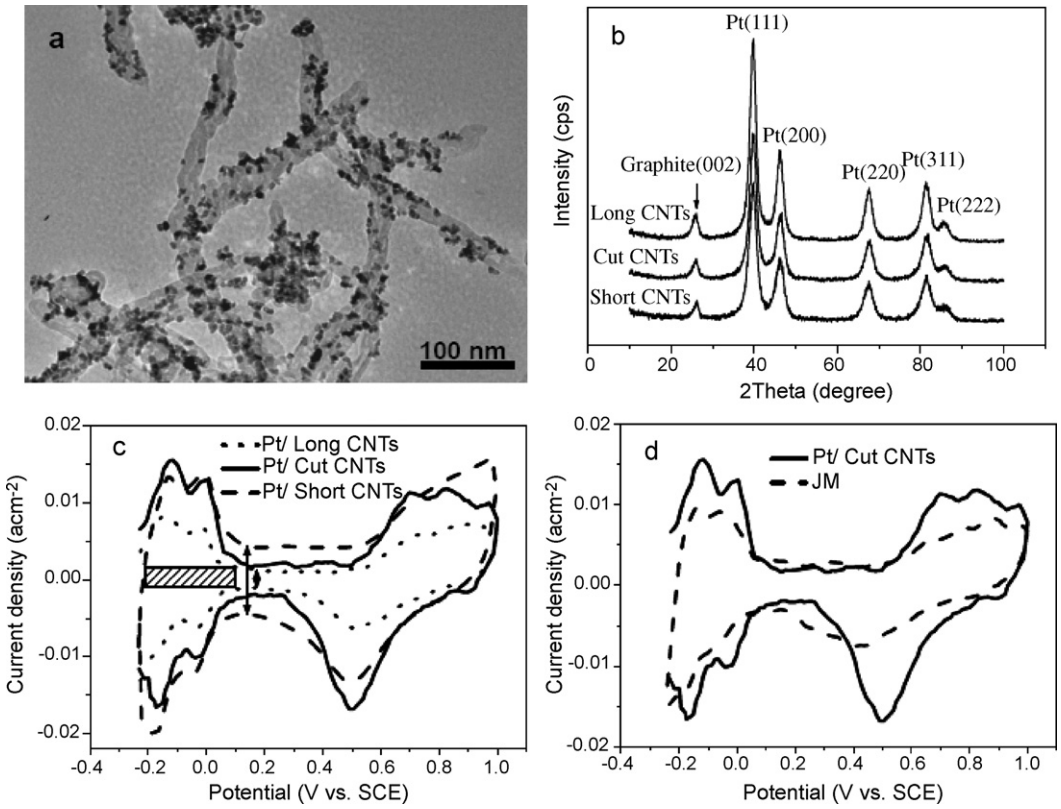

Fig. 6. Results of catalysts based on long, short and cut CNTs. (a) TEM image of Pt particles deposited on short CNTs, (b) XRD patterns of all catalysts, (c) cyclic voltamograms of the three catalysts, and (d) comparison between the present and commercial (JM) catalysts. The Pt loading on each electrode was 0.4 mg cm^{-2}, and the potential sweep rate was 100 mV s^{-1}. The electric double layer is arrowed in (c), and the shaded area represents the contribution of the double layer charge to the overall amount of charge exchanged during the electro-adsorption/desorption of H_2 on Pt sites. Similar markings can be applied for other catalysts in both (c) and (d).

surface area of the Pt catalyst based on short CNTs is much larger than that based on long CNTs (see Table 1). Furthermore, the present catalyst illustrates an apparently higher activity than the commercial catalyst from Johnson Matthey (JM) Co. (Fig. 6d).

As a support for Pt catalyst, short CNTs also show better performance than long CNTs. The reason for this may be that the CNTs with short length prepared here can be well dispersed in solution. This is an important requirement for uniform deposition of Pt nanoparticles on the surface of CNTs and for uniform deposition of the catalyst particles on the electrode. Severe entangling of long CNTs usually leads to the opposite results. Furthermore, shorter CNTs have a lower stacking density and thus more secondary pores. These secondary pores may provide more channels for electrolyte, and facilitate the diffusion of H^+ in the catalyst layer to contact with Pt nanoparticles. As a result, the utilization ratio of Pt nanoparticles is sharply enhanced (Table 1), and the electrochemical activity is improved.

4. Conclusions

In conclusion, CNTs with ultra-short length of about 300 nm, high dispersion and high purity can be prepared from direct growth. The direct growth involves in situ formation of the catalyst of FeS. This iron compound may retard dissolution and diffusion of carbon when compared with pure Fe, and thus play a key role in limiting the length of CNTs. The present short CNTs from direct growth have the same characters as the short ones from solid-state cutting, and both show much better performance as an electrode material in Li-ion batteries and as a catalyst support in fuel cells than conventional long CNTs. The present synthetic technique may be used for mass production of short CNTs to be applied in wide areas.

Acknowledgements

JNW thanks The Outstanding Youth Fund and the research project of 50871067 from The National Natural Science Foundation of China and the national 863 project of 2007AA05Z128 from the Ministry of Science and Technology of China.

References

[1] S. Iijima, Nature 354 (1991) 56–58.
[2] H.J. Dai, Surf. Sci. 500 (2002) 218–239.
[3] S. Subramoney, Adv. Mater. 10 (1998) 1157–1171.
[4] B. Gao, C. Bower, J.D. Lorentzen, L. Fleming, A. Kleinhammes, X.P. Tang, L.E. McNeil, Y. Wu, O. Zhou, Chem. Phys. Lett. 327 (2000) 69–74.
[5] À. Kukovecz, T. Kanyó, Z. Kónya, I. Kiricsi, Carbon 43 (2005) 994–1000.
[6] I. Stepanek, G. Maurin, P. Bernier, J. Gavillet, A. Loiseau, R. Edwards, O. Jaschinski, Chem. Phys. Lett. 331 (2000) 125–131.
[7] Z. Gu, H. Peng, R.H. Hauge, R.E. Smalley, J.L. Margrave, Nano Lett. 9 (2002) 1009–1013.
[8] J. Liu, A.G. Rinzler, H. Dai, J.H. Hafner, R.K. Bradley, P.J. Boul, A. Lu, T. Iverson, K. Shelimov, C.B. Huffman, F. Rodriguez-Macias, Y.S. Shon, T.R. Lee, D.T. Colbert, R.E. Smalley, Science 280 (1998) 1253–1256.
[9] Z.J. Jia, Z.Y. Wang, J. Liang, B.Q. Wei, D.H. Wu, Carbon 37 (1999) 903–906.
[10] X.X. Wang, J.N. Wang, L.F. Su, J.J. Niu, J. Mater. Chem. 16 (2006) 4231–4234.
[11] X.X. Wang, J.N. Wang, Carbon 46 (2008) 117–125.
[12] S.S. Fan, L. Liu, M. Liu, Nanotechnology 14 (2003) 1118–1124.
[13] N.M. Rodriguez, J. Mater. Res. 8 (1993) 3233–3251.
[14] H.J. Dai, A.G. Rinzler, P. Nikolaev, A. Thess, D.T. Colbert, R.E. Smalley, Chem. Phys. Lett. 260 (1996) 471–475.
[15] H.M. Cheng, F. Li, G. Su, H.Y. Pan, L.L. He, X. Sun, M.S. Dresselhaus, Appl. Phys. Lett. 72 (1998) 3282–3284.
[16] L.J. Ci, J.Q. Wei, B.Q. Wei, J. Liang, C.L. Xu, D.H. Wu, Carbon 39 (2001) 329–335.
[17] R.T.K. Baker, Mater. Res. Soc. Symp. Proc. 349 (1994) 251–256.
[18] S. Maruyama, R. Kojima, Y. Miyanchi, S. Chiashi, M. Kohno, Chem. Phys. Lett. 360 (2002) 229–234.
[19] H. Kataura, Y. Maniwa, T. Kodama, K. Kikuchi, K. Hirahara, K. Suenaga, S. Iijima, S. Suzuki, Y. Achiba, W. Krätschmer, Synth. Met. 121 (2001) 1195–1196.